



Originally published as:

Uhlenbrook, S., Didszun, J., Wenninger, J. (2008): Source areas and mixing of runoff components at the hillslope scale - a multi-technical approach. - Hydrological Sciences Journal - Journal des Sciences Hydrologiques, 53, 4, 741-753

DOI: [10.1623/hysj.53.4.741](https://doi.org/10.1623/hysj.53.4.741)

1 **Source areas and mixing of runoff components at the hillslope**
2 **scale – A multi-technical approach**

3 **STEFAN UHLENBROOK^{1,2}, JENS DIDSZUN³ & JOCHEN WENNINGER⁴**

4 ¹ UNESCO-IHE, Department of Water Engineering, PO Box 3015, 2601 DA Delft, The
5 Netherlands, s.uhlenbrook@unesco-ihe.org

6 ² Delft University of Technology, Department of Water Resources, PO Box 5048, 2600
7 GA Delft, The Netherlands

8 ³ GeoForschungsZentrum Potsdam, Section 5.4, Telegrafenberg, D-14473 Potsdam,
9 Germany

10 ⁴ University of Freiburg, Institute of Hydrology, Fahrenbergplatz, D-79098 Freiburg,
11 Germany

12

13 **Abstract** Hillslope processes (i.e. water flow pathways, source areas and residence times)
14 are essential for predicting water quantities and water quality. A multi-technical approach
15 using classical hydrometry, natural and artificial tracers and electrical resistivity
16 tomography (ERT) was applied to two adjacent steep hillslopes in the Black Forest
17 Mountains, Germany. The differences in the hydrological and hydrochemical responses
18 during three floods were larger than expected based on previously available information
19 of topography, land use and geology. At one site a very dynamic shallow groundwater
20 system dominated the flood generation, which could not be observed at the other site. The
21 reasons for the heterogeneity of hillslope processes are the different soils and structures
22 of the peri-glacial drift (first-order control); this is augmented by the different land use

23 (pasture vs. forest) and its effects on the near-surface processes (second-order control).
24 The multi-technical approach proved very useful: The tracer methods enabled the
25 detection and quantification of runoff components; geophysical methods provided further
26 insights into the subsurface structure and, consequently, the origin of runoff components.

27

28 **Résumé** Les processus hydrologiques à flanc de coteau (p.ex. cheminements d'eau, zones
29 d'origine et temps de séjour) sont importants à prévoir la qualité et quantité des eaux. Les
30 mesures hydrométriques classiques, traceur naturel et artificiel ainsi que tomographie de
31 résistivité électrique (TRE) ont été combiné dans deux versants avoisinant dans la
32 montagne Forêt-Noir, en Allemagne. Les différences entre les réponses hydrologiques et
33 hydrochimiques durant trois crues étaient plus grand qu'attendu à base des informations
34 disponibles du topographie, gestion de terroir et géologie. Dans l'un des versants, un
35 écoulement souterrain superficiel très dynamique pouvait être observé qui n'était pas
36 présent dans l'autre. L'hétérogénéité des processus hydrologiques à flanc de coteau peut
37 être attribuée aux sols divers et aux structures périglaciaires du sédiment (contrôle de
38 premier ordre); elle est encore augmentée par les différentes gestions de terroir (pâturage
39 versus forêt) et leurs effets sur les processus superficiels (contrôle de deuxième ordre).
40 L'utilisation combinée de différentes techniques s'est démontrée très utile : Les études de

41 traceur ont permis de découvrir et quantifier les composantes de l'écoulement; L'étude
42 TRE a permis de mieux comprendre la structure du sous-sol et par conséquent l'origine
43 des composantes de l'écoulement.

44

45 **Key words** hillslope hydrology, environmental tracers, electrical resistivity tomography
46 (ERT), Black Forest Mountains

47 **Mots clefs** hydrologie des pentes de collines, traceurs environnementaux, tomographie de
48 résistivité électrique (IRE), montagne Forêt-Noire

49

50 **INTRODUCTION**

51 Understanding hillslope processes, in particular water flow pathways, source areas and
52 residence times, is essential for predicting water quantities (incl. floods and low flows)
53 and water quality in a catchment (e.g. Bonell, 1998). Recently considerable advances in
54 hillslope process understanding have been achieved (e.g. Anderson & Burt, 1990;
55 McDonnell & Tanaka, 2001), which contributed to a conceptual process knowledge at the
56 hillslope and small catchment scale. However, a unifying and generalized theory of
57 process functioning across different hillslope types is still missing (McDonnell, 2003).
58 This is necessary to improve process-based modelling at the hillslope scale in order to

59 improve the predicting of the impact of changes (e.g. land use change, climate change) on
60 the hydrological response of a catchment.

61 Hillslope processes within a small catchment, which hydrological and
62 hydrochemical responses are mainly controlled by hillslopes, define how precipitation
63 reaches the stream, how long water is stored as surface water, soil water and groundwater
64 systems, and what hydrochemical composition these components have. To explore
65 hillslope processes different methods have been developed. They range from classical
66 comparisons of rainfall/runoff relationships, soil physical studies, sprinkling experiments,
67 tracer studies using artificial and natural tracer to geophysical measurements (e.g.
68 Anderson and Burt, 1990; Montgomery *et al.*, 1997, Jones, 2000; Tromp-van Meerfeld &
69 McDonnell, 2006; Scherrer *et al.*, 2007). Each method has its strengths and shortcomings
70 concerning costs and the temporal and spatial scale at which it can be used.
71 Unfortunately, in most studies only one or two methods were used to investigate hillslope
72 processes and this limits the complete understanding of the complex processes.

73 Use of natural tracers demonstrated that the retention of water in small catchments
74 can be very long (e.g. Kirchner *et al.*, 2000; McGuire & McDonnell, 2006). However,
75 where and how the water is stored for so long, while the hydrodynamic reaction can be
76 very quick (c.f. 'hydrological paradox'; Kirchner, 2003) is not completely understood.

77 Uhlenbrook *et al.* (2002) showed similar behaviour for the 40 km² Brugga catchment in
78 the Black Forest Mountains, Germany. Here the so-called shallow groundwater is the
79 most important runoff component (about 70% of total runoff) that contributes also
80 significantly to flood formation, but the mean residence time of the water was estimated
81 to 2-3 years. Where this water is stored in the catchment, and how it can be mobilized
82 quickly during high flows is not well understood. Thus, new experimental techniques
83 need to be developed to gain a better understanding in particular of subsurface flow
84 processes (e.g. Beven, 2005; Uhlenbrook, 2006). To what extent multi-technical
85 approaches using the latest developments in hydrogeophysics (Hubbard & Rubin, 2005)
86 together with classical hydrometric methods and tracer methods might help to decipher
87 subsurface flow processes is a current challenge in hillslope hydrology.

88 The objective of this paper is to investigate the runoff generation processes at two
89 neighboring, steep hillslopes using a combination of different experimental techniques:
90 rainfall and spring discharge measurements, different natural and artificial tracers and
91 electrical resistivity tomography (ERT). The specific objectives were (i) to quantify the
92 contributions of runoff components during different hydrological situations (floods and
93 low flows), (ii) to identify the source areas of the runoff components, and (iii) to compare
94 the results of two hillslopes with the aim to identify generalizable mechanism.

95

96 **MATERIAL AND METHODS**

97 **Study sites**

98 The two hillslopes are located in the Brugga catchment, Southern Black Forest
99 Mountains, Germany, (Fig. 1). It is a low mountain range, 40 km² catchment with an
100 elevation range of 438-1493 m and roughly the following water balance values:
101 precipitation 1750 mm a⁻¹, discharge 1230 mm a⁻¹ and evaporation 520 mm a⁻¹. The
102 bedrock consists of gneiss and is covered by a glacial and periglacial drift and debris
103 cover of varying depths (0-10 m). Brown soils (cambisols) have mainly developed in this
104 drift cover and their texture is loamy sand with a high stone content (10-30%). There are
105 many macropores in the soils, i.e. root channels and earth worm channels. However, an
106 extended soil pipe network, which could be crucial for the hydrological response (e.g.
107 Jones, 2004), could not be found.

108 Both test sites are quite similar regarding their geology, altitude, catchment area,
109 length and inclination. They are steep with a mean slope of 25° and 24° for the lower
110 hillslope above the springs A and B, respectively (Fig. 1). Both springs, namely
111 Zipfeldobel (spring A) and Zaengerlehof (spring B), are located at the toe of the
112 hillslopes and initiate a little creek, which is at both sites directly connected to the next

113 stream. The depth of the bedrock is not exactly known, but because of the
114 geomorphological context and topographic position (cf. Fig. 1) it has to be assumed that
115 the bedrock is at least 10 m below the surface at both sites. The land use differs at both
116 sites and is dominated by pasture land and spruce forest at hillslope A and B,
117 respectively. The infiltration rates are at both sites higher than the recorded rainfall
118 intensities; infiltration excess overland flow could not be observed since experimental
119 investigations started in 1998.

120 Recent investigations in the Brugga and sub-catchments using tracers
121 (Uhlenbrook *et al.* 2002; Didszun & Uhlenbrook, 2007) identified three main flow
122 systems: (i) Fast runoff components (surface and near-surface runoff) are generated at
123 sealed or saturated areas and on steep highly permeable slopes covered by boulder fields.
124 The average contribution of this component was estimated to 10%, but it can be up to
125 50% during floods. (ii) Base flow components (deep groundwater) originate from the
126 fractured hard rock aquifer and the deeper parts of the weathering zone (average
127 contribution about 20%). (iii) An intermediate flow system (shallow groundwater)
128 originates mainly from the periglacial drift and debris cover of the slopes (average
129 contribution about 70%). The hydrochemistry clearly indicates that shallow groundwater
130 contributes during floods and low flow. The mean residence time was estimated to two to

131 three years, determined by ^{18}O measurements. Generally little is known about the depth,
132 permeability and storage characteristics of the soils and periglacial drift material.

133

134 **Field and laboratory work**

135 *Hydrometry and tracers* The spring discharges at site A and B were monitored using
136 electromagnetic flow meters (produced by ‘Krohne’) for the period 1998-2004 and 1999-
137 2004, respectively. Unfortunately, the time series are very scattered and these periods
138 were interrupted for many times due to technical measurement problems. A climate
139 station that measures precipitation (10-minutes interval) is about 2 and 4 km away from
140 site A and B, respectively; it is at about the same elevation as the mean of the spring
141 catchments. During the investigation period in fall 1999 one additional rain gauge was
142 located close to spring A. Water samples were taken regularly on a weekly/bi-weekly
143 basis. In addition, samples were taken at each spring in a 4-hour time interval using
144 automatic samplers during an intensive measurement campaign in fall 1999. During that
145 campaign water samples were analysed for deuterium (^2H), dissolved silica and major
146 anions (Cl^- , NO_3^- , SO_4^{2-}) and major cations (Na^+ , K^+ , Ca^{2+} , Mg^{2+}). Rainwater was
147 sampled every 2 mm and analysed for deuterium to observe the intra-storm variability.

148 The anions and cations were analysed by ion exchange chromatography with a
149 DIONEX DX 500 device; a mean analytical error of 3% was determined. Dissolved silica
150 concentrations (referred to as silica in the following text) were determined by
151 photometric measurements according to the German Institute for Standardization
152 DIN 1981; the mean analytical error was approximately 1%. Deuterium (^2H) was
153 analysed using a Finnigan MAT Delta S dual inlet isotope ratio mass spectrometer
154 (IRMS) with an H-device (chrome reduction method at 900°C). The isotope values are
155 given as δ -values [‰] referring to the international standard Vienna Standard Mean
156 Ocean Water (VSMOW). Analytical precision was better than $\pm 1\%$. The fluorescence
157 tracers Naphthionat and Uranine were analysed with a spectral fluorometer (Perking
158 Elmer); the analytical error amounted to 2 %. Bromide, additionally used as artificial
159 tracer, was also analysed with the ion chromatograph.

160 Two- and three-component hydrograph separations were used to separate the
161 storm flow hydrograph. This technique is based on the mass balance of water and tracer.
162 The fundamentals and assumptions are discussed extensively in the literature (e.g. Buttle
163 1994).

164

165 ***Electrical resistivity tomography (ERT)*** Electrical resistivity surveys are a standard
166 method in geology or geotechnical investigations; nowadays the method is used more
167 frequently in environmental hydrology (e.g. Binley *et al.*, 1996, Cosmas et al., 2004;
168 Hubbard & Rubin, 2005). The subsurface resistivity is related to geological and
169 hydrological parameters like rock/soil type, grain sizes, porosity as well as the pore fluid
170 properties (Loke, 2003). The determination of subsurface resistivity is based on Ohm's
171 law, which describes the relationship between the current density, the electrical field
172 (voltage) and the resistivity (e.g. Loke, 2003). In order to map the electrical resistivity of
173 the subsurface, a current is induced between two current electrodes and the resultant
174 potential field is measured at two separate potential electrodes. The survey configuration
175 used in this study was an electrical resistivity tomography (ERT), which combines
176 surface profiling and vertical sounding into a 2-D image of the subsurface resistivity
177 (Loke, 2003; Binley & Kemna, 2005).

178 The resistivity surveys were carried out using the Syscal Junior Switch System
179 with two multi-core cables with 24 electrode outlets. The spacing between the electrodes
180 varied between 1 to 5m, what provided results in an appropriate spatial resolution to
181 varying depth. The electrodes were set along hillslope transects (Fig. 1), and a 'roll along
182 procedure' (installing half of the electrodes at the end of the transect as soon as the first

183 half of the electrodes are free) enabled to investigate transects with more than 24
184 electrodes. A Wenner configuration was used as the electrical array. All measurements
185 were carried out during similar moisture conditions in summer 2004. The measured
186 pseudosections (apparent resistivity) were processed with a 2-D inverse numerical
187 modeling technique (software: Res2Dinv) to give the estimated true resistivities of the
188 subsurface (for further details see e.g. Loke, 2003).

189

190 **RESULTS AND DISCUSSION**

191 **Rainfall/runoff observations**

192 The observed discharges were in the ranges $0.26\text{-}2.3 \text{ l s}^{-1}$ and $0.32\text{-}1.3 \text{ l s}^{-1}$ and mean
193 discharges were estimated to 0.56 and 0.51 l s^{-1} for spring A and B, respectively. These
194 values were estimated from the remaining records of the whole time series after data
195 quality control. During the whole investigation period both springs had a stable base flow
196 of about $0.3\text{-}0.4 \text{ l s}^{-1}$. These facts indicate that both catchment sizes are similar (both
197 areas get about the same average precipitation); however, they could not be determined
198 accurately because of the steep topography.

199 Clear differences between the springs' hydrographs can be observed during
200 rainfall events in autumn 1999 (Fig. 2). These events occurred during relatively dry

201 antecedent conditions after a warm summer. The first events at both springs are
202 independent from the last rainfall event that occurred 14 days before and amounted to
203 only 11.7 mm; the rainfall since then are given in table 1. Spring A is characterized by
204 slow and delayed runoff behaviour. In contrast, the time lag of the runoff response at
205 spring B is shorter, the peak discharge is higher and its maximum is reached about two
206 days earlier. The runoff recession is considerably steeper at spring B than at spring A.
207 The rapid runoff response and the fairly constant base flow discharge at spring B suggests
208 that this spring is fed by at least two runoff components, a long-lasting base flow
209 component and a dynamic storm flow component.

210 Significant differences in precipitation at both hillslopes were observed during the
211 events 2a and 3 (table 1); events 1 and 2 were rather equal. To compare the runoff
212 responses during the events, the runoff volumes and the ratios of runoff volumes divided
213 by precipitation were calculated (table 1). The latter parameter can be interpreted as a
214 kind of runoff coefficient, which could not be estimated directly because of the unknown
215 catchment area. At spring A, event runoff volumes were calculated by summing up the
216 discharge increase (discharge minus pre-event discharge) from the beginning of the
217 runoff event till the beginning of the next event. It could not be calculated for event 2a
218 (minor discharge increase), and the values are given in brackets for event 3 as the

219 increase in discharge was small and the pre-event runoff was high. At spring B, the event
220 discharge volume (discharge minus pre-event discharge) could be estimated clearly for
221 events 1, 2 and 3 considering the period from the beginning of the rising limb till the
222 sharp end of the peak flow hydrograph. For event 2a, the summation was stopped when
223 the discharge reached pre-event values.

224 Although the estimation of the event discharge volumes has some uncertainty, it
225 enables a comparison of the runoff responses between the three events at each spring. It
226 has to be noted that the discharge volume/precipitation ratios cannot be compared directly
227 between the two springs. However, the ratio values suggest that there are thresholds at
228 both springs that trigger a significant increased runoff generation once this threshold is
229 exceeded. Small storm events (e.g. event 2a) cause almost no response in the hydrograph
230 at spring A and a significantly lower discharge volume at spring B. Qualitatively this
231 threshold behaviour could be confirmed considering events in subsequent years.
232 Unfortunately, the threshold could not be estimated more accurately due to uncertainties
233 of the real rainfall input (e.g. rain gauge at hillslope A was only available during the
234 measurement campaign in fall 1999) and the poor discharge data quality due to technical
235 measurement problems.

236

237 **Tracer results**

238 *Hydrochemical and tracer measurements* At spring A, the concentration of dissolved
239 silica remained fairly constant throughout the events 1-3 (Fig. 3). Only towards the end of
240 the recession of each event, a minor decrease of the silica concentrations was detected.
241 The concentrations of the major anions and cations showed the same response, the
242 concentrations remained constant during the events (Fig. 4).

243 At spring B, a typical decrease in the silica concentrations was observed (Fig. 3)
244 that was synchronous with the peak discharge for all investigated events. The silica
245 concentration dropped to about 70 % of the pre-event concentration and reached the pre-
246 event concentration again at the end of the hydrograph recession. No significant change
247 in concentrations during the small event 2a could be detected. The concentration changes
248 of the major anions and cations had a similar pattern, the concentrations dropped to a
249 minimum of about 50 % of the pre-event concentration (Fig. 4). This decrease in
250 concentrations indicates the significant contribution of at least one additional storm
251 runoff component, which is hydro-chemically different from the base flow producing
252 groundwater. The hardly detectable concentration changes at spring A do not indicate to
253 the contribution of an additional storm runoff component. These hydro-chemical

254 reactions are in line with the observed hydrological behaviour of the two springs during
255 the events.

256 Also the isotopic composition of the spring water during all events illustrated the
257 marked differences of the two investigated systems. At spring A only negligible
258 variations in the deuterium composition were observed (Fig. 5). At spring B a change of
259 the deuterium signature towards isotopically more heavy water (higher δ -values) was
260 determined, even if isotopic signature of the precipitation was predominantly lighter
261 (lower δ -values) than present groundwater (Fig. 5). This suggests the contribution of a
262 third runoff component that has a different isotopic composition compared to the event
263 and pre-event components. It is interesting to note, that these patterns are similar for the
264 three investigated events. The high δ -values during peak discharge at spring B indicate
265 that the third runoff component was recharged during the summer times (characterized by
266 isotopically heavy precipitation).

267

268 ***Hydrograph separations*** To quantify the contribution of the different runoff components
269 to spring discharge during events two- and three-component hydrograph separations were
270 carried out using dissolved silica and deuterium as natural tracers. It is important to note

271 that the same results were observed for the other events shown in figure 2, which are not
272 discussed in further detail here.

273 At spring A, two-component hydrograph separation using dissolved silica resulted
274 in a minor contribution of direct runoff of about 3% during the observed events (Fig. 6),
275 which caused the small decrease in silica concentration (Fig. 3). Therefore, it was
276 supposed that spring discharge consists of two components (i) direct runoff (assumed
277 silica concentration: 0.3 mg l^{-1}) and (ii) groundwater (assumed silica concentration: 6.1
278 mg l^{-1} ; estimated from samples taken prior to the event). The small proportion of direct
279 runoff could reach the spring during the event by flowing along preferential pathways
280 (i.e. root channels, earthworm channels, etc.). The rest of the spring water was delivered
281 from groundwater; a further distinction into for instance shallow and deep groundwater
282 (cf. Uhlenbrook *et al.*, 2002) was not possible.

283 A two-component hydrograph separation could also be calculated assuming a
284 variable contribution of two groundwater components that changed their relative
285 contributions during the event, i.e. an increase of the component with lower silica
286 concentrations. However, available data did not allow to determine different silica
287 concentrations, thus an estimation of the fraction of each component would become
288 arbitrary and uncertain.

289 At spring B, a two-component hydrograph separation was not feasible, as the
290 deuterium concentrations indicated a third component (see above, Fig. 5). Thus, a three-
291 component separation was calculated using silica and deuterium as tracers. The three
292 components are (i) direct runoff, with low silica concentrations and the deuterium
293 composition of rainwater (temporal variable, incremental mean according to McDonnell,
294 1990), (ii) shallow groundwater and (iii) deep groundwater. The deuterium and silica
295 concentrations for the deep and shallow groundwater (Fig. 7) were determined using end
296 member mixing diagrams according to Christophersen *et al.* (1990), because it was not
297 possible to measure the concentrations directly. The results demonstrate that shallow
298 groundwater already contributed a small proportion of base flow prior to the events, and
299 became the major component during the peak of the event (Fig. 6). During the three
300 investigated events, the fraction of the direct runoff component was about 10%, whereas
301 the deep and shallow groundwater made up approximately 40% and 50%, respectively.

302

303 ***Artificial tracer experiments*** Artificial tracers were injected at 12 October 1999 in
304 different distances uphill from the springs to mark flow paths. The experimental set up
305 was the same at both sites: (i) 5 kg sodium bromide (NaBr) were injected 10 m uphill as
306 line injection in a small trench (0.3x1.5 m, about 0.2 m deep). (ii) 2 kg of the

307 fluorescence dye Naphthionat were injected about 19 m uphill in a similar small trench.
308 (iii) 0.15 kg of the fluorescence dye Uranine was injected in hand-drilled wells at depths
309 of about 1 m. The objective was to trace the flow paths of the infiltrating water near
310 spring outlet with the first two injections. The last injections should have excluded a
311 possible retention in upper soil (A-horizon, large porosity) and trace the lateral flow paths
312 below the root zone. Only limited amounts of water were applied before (few litres) and
313 after (a few 10s of litres) the injection not to push the tracer through the system, but to
314 mimic the natural flow driven by infiltration, percolation and lateral flow.

315 In contrary to the discharge responses during events since mid October and the
316 contribution of direct runoff, in particular at spring B, no artificial tracers were found in
317 the spring water for the following two months. Only bromide could be found at both
318 springs at the same time after 8 weeks. A peak in bromide concentration could be
319 detected at spring A during a larger flood event (peak flow 1.7 l s^{-1} at spring A, 19
320 December). The bromide breakthrough at spring B was unsteady with significant
321 variations in tracer concentrations in the samples. None of the fluorescence dyes could be
322 detected except for some Uranine dye at spring B 15 days after the first bromide
323 breakthrough. Uranine could be detected over six weeks but the concentrations were
324 close to the detection limit.

325

326 **Geophysical observations**

327 The ERT measurements resulted in distinct different resistivity patterns at both sites
328 (Figures 8 and 9). At the hillslope above spring A, the electrical resistivity values indicate
329 a relatively thick and homogeneous zone ($> 1000 \Omega\text{m}$; unsaturated zone confirmed by
330 auger holes) above the phreatic zone ($< 500 \Omega\text{m}$) that feeds the spring at the toe of the
331 hillslope. The assumed saturation of the latter zone is in line with many other ERT
332 measurements in the area with ground truth data.. The low resistivity area reaches 30 m
333 upslope a depth of more than 10 m, suggesting a large unsaturated zone (Fig. 8). We
334 interpret from this that the infiltrating rainwater needs to flow predominantly vertically
335 through the unsaturated zone before it reaches the groundwater that flows laterally. The
336 groundwater table rise causes a displacement of groundwater stored at the spring outlet
337 (prevent groundwater). A shallow groundwater body (at less than 5 m depth) could not be
338 detected at this site and rapid lateral subsurface flow was not evident (cf. tracer data
339 above).

340 At the hillslope above spring B a significantly higher range of resistivity values
341 was observed near the soil surface a few tens of meters uphill. The high values indicate a
342 more heterogeneous subsurface structure including coarser bedrock material (boulders).

343 Areas of lower resistivities ($<500 \Omega\text{m}$) could be found near the location of the spring and
344 also 60 m upslope relatively close to the surface (Fig. 9). It can be concluded that
345 infiltrating rainwater can reach the shallow hillslope groundwater quicker as it is
346 shallower, and accordingly causes groundwater displacement at the spring outlet.

347 One limitation during the interpretations of the geoelectrical patterns is the lack of
348 borehole data for ground truthing on site. Several attempts to drill holes of a depth of
349 more than 1m (using a hand auger) failed because of the steepness of the terrain, the
350 occurrence of big stones/block in the drift cover and the dense forest at spring B. The
351 interpretations about saturated/unsaturated conditions were based on experiences gained
352 from ERT measurements near the study areas with the same geology (unpublished data)
353 and could be supported by surficial characteristics (i.e. wetness indicating plants, boulder
354 etc.), a geological map (1:25,000) and a forest site map (1:10,000). However, a definite
355 statement about saturated conditions could not be made as the subsurface resistivity is
356 related to geological and hydrological parameters (i.e. rock/soil type, grain sizes, porosity
357 and pore fluid properties). In spite of the uncertainties, the data provides further
358 descriptive insights of subsurface structures and water occurrence. The detection of low-
359 resistivity areas ($<500 \Omega\text{m}$) uphill of spring B can under the given assumptions be
360 interpreted as a shallow, inclined groundwater body. This fits nicely to the results of the

361 hydrograph separation using dissolved silica and environmental isotopes, which
362 demonstrated a highly dynamic shallow groundwater body.

363 The resistivity patterns at both sites display areas with relatively large ohm-meter
364 values at 10-20 m uphill of the springs. This indicates that there is a quite large
365 unsaturated zone storage, exactly where the artificial tracers were injected. We interpret
366 that the tracers got stuck there and first needed to be transported through percolating
367 water into greater depths before they were transported laterally to the spring outlet.
368 Therefore, sufficient rainfall was needed as transport medium, note that bromide could
369 only be detected in connection to a large event more than two months after the event. The
370 fact that none of the fluorescence dyes could be detected can not be fully explained with
371 the existing information, but might be caused by a bypass of groundwater that initiate a
372 wetland close to the spring outlet.

373

374 **Synthesis**

375 Runoff generation processes at the two sites differ to a larger extent than it would be
376 expected from the previously available geological and topographic information as well as
377 surface characteristics, i.e. the similar locations of the springs at the toe of two steep
378 hillslopes that consist of the similar bedrock material according to the geological map.

379 The reasons for the different hydrological and hydrochemical responses could be
380 attributed primarily to different structures of the debris and drift cover at the hillslopes
381 above each spring. The direct impact of the land use is obvious in the upper soil, as the
382 porosity and hydraulic permeability can be quite different in the root zone under grass
383 land (hillslope A) and conifers (hillslope B). For the latter, the root network goes deeper
384 and has generally more and longer (connected) preferential flow pathways, which could
385 enable a quick percolation and delivery of shallow subsurface water to spring B.
386 However, it is surprising that the artificial tracer tests, which were designed to proof
387 exactly the impact of the near-surface flow pathways, yielded exactly the same results.
388 Consequently, it is wrong to attribute the striking hydrological and hydrochemical
389 differences at both sites to the land use only.

390 The ERT measurements served as an ‘eye-opener’, as they provided insights into
391 the differing structures of the sub-surface and the location of phreatic zones. They helped
392 to explain the surprisingly slow tracer transport and located the source area of the rapid
393 subsurface flow component at spring B. This is a major step as the hydrochemical
394 observations and hydrograph separations were useful to detect and quantify the
395 contribution of the two and three components during flood runoff at both sites, but the
396 origin and flow pathways remained unspecified.

397 Combining all techniques leads to the following conceptual model of runoff
398 generation: Classical infiltration excess overland flow plays no role at both sites, and
399 flood runoff was produced to 90 % and more by soil and groundwater displacement. At
400 spring B a highly dynamic shallow groundwater component dominated the generation of
401 flood runoff during all events. The isotope data indicate that this was recharged some
402 months ago. If an extended soil pipe system (e.g. Jones, 2004; Weiler & McDonnell,
403 2007) is important for the quick flow of this component could not be proved. The shallow
404 groundwater could not be observed at spring A, which is due to different structure of the
405 drift cover. The fact that only minor contributions of direct runoff could be detected
406 demonstrates an extensive mixing of event water with water stored in the soil and drift
407 cover prior to the event (cf. McDonnell, 1990). The runoff generation processes seem to
408 be accelerated by increasing precipitation volumes and intensities, only after exceeding a
409 certain threshold a significant rise in the discharge volumes was detectable at both
410 springs. The conifers and the larger permeability of the upper soil at hillslope B most
411 likely made a quick recharge and displacement of shallow subsurface possible. However,
412 the quick and substantial generation of this runoff component is caused by the drift and
413 debris cover structure and not only by the land use.

414

415 **CONCLUSIONS**

416 The combination of a classical hydrometric approach with hydrochemical and tracer
417 investigations as well as a geophysical method proved very useful to provide further
418 insights into the generation and origin of different runoff components at the hillslope
419 scale. The tracers enabled to detect and quantify the contribution of runoff components.
420 The electrical resistivity patterns of the subsurface allowed us 'to see' the heterogeneity
421 of the subsurface structure, and helped to locate the source areas of the runoff
422 components. Combining the techniques allowed developing a conceptual understanding
423 of runoff generation at the test sites.

424 As shown for the two investigated hillslope/spring systems, the hydrological
425 processes and flow pathways at a mountainous test site can be very diverse, even at
426 hillslopes that appeared similar from their general physiographic characteristics. The
427 heterogeneity of hillslope processes is caused by the different soil and drift structures in
428 the shallow subsurface (first-order control) and augmented by the land use and its effects
429 on the near-surface processes (second-order controls). As detailed information on the
430 first-order control is usually not available, a regionalisation of processes based on
431 nowadays existing spatial data sets as, for instance, topography, land use, soil maps
432 (usually restricted to the upper soil) or regional geology, is very uncertain. A better

433 knowledge of the subsurface structure in first meters (incl. layering and hydraulic
434 conductivity) would be needed in such environments.

435

436 **Acknowledgements** The project was supported by the German Research foundation
437 (grant number Le 698/12-3). The geophysical equipment was financed by a grant for
438 especially talented post-docs by the state of Baden-Württemberg, Germany. Special
439 thanks to Prof. Chris Leibundgut (University of Freiburg, Germany) who supported the
440 research in many ways.

441

442 **References**

443 Anderson, M. G. & Burt, T. P. (1990) *Process studies in hillslope hydrology*. Wiley, Chichester,
444 UK.

445 Beven, K. J. (2005) *Streamflow Generation Processes*. Benchmark Papers in Hydrology, IAHS
446 series, No. 1.

447 Bonell, M. (1998) Selected challenges in runoff generation research in forests from the hillslope
448 to headwater drainage basin scale. *J. of American Wat. Resour. Assoc.* **34**(4), 765–785.

449 Binley, A., Shaw, B., & Henry-Poulter S. (1996) Flow pathways in porous media: electrical
450 resistance tomography and dye staining image verification. *Meas. Sci. Technol.* 7, 384-390,
451 doi:10.1088/0957-0233/7/3/020

452 Binley, A. & Kemna, A. (2005) Resistivity and Induced Polarization Methods. In:
453 *Hydrogeophysics* (ed. by Rubin, Y. & Hubbard, S.), 129-156, Springer, Dordrecht, The
454 Netherlands.

455 Buttle, J. M. (1994) Isotope hydrograph separations and rapid delivery of pre-event water from
456 drainage basins. *Progr. in Phy. Geogr.* **18**, 16-41.

457 Comas, X., Slater, L. & Reeve, A. (2004) Geophysical evidence for peat basin morphology and
458 stratigraphic controls on vegetation observed in a Northern Peatland. *J. Hydrol.* **295**, 173-184.

459 Christophersen, N., Neal, C., Hooper, R. P., Vogt, R. D. & Andersen, S. (1990) Modelling stream
460 water chemistry as a mixture of soil water end-members - a step towards second-generation
461 acidification models. *J. Hydrol.* **116**, 307-320.

462 Didszun, J., Uhlenbrook, S. (2007) Impacts of catchment scale on runoff components – a tracer
463 based approach. *Wat. Resour. Res.*, in press.

464 Hubbard, S. S. & Rubin, Y. (2005) Introduction to Hydrogeophysics. In: *Hydrogeophysics* (ed. by
465 Rubin, Y. & Hubbard, S.), 3-21, Water Science and Technology Library, vol. 50, Springer,
466 523 p.

467 Jones, J. A. (2000) Hydrologic processes and peak discharge response to forest removal,
468 regrowth, and roads in 10 small experimental basins, western Cascades, Oregon. *Wat.*
469 *Resour. Res.* **36**(9), 2621-2642.

470 Jones, J. A. A. (2004) Implications of natural soil piping for basin management in the British
471 uplands. *Land Degradation and Development* **15**(3), 325-349.

472 Kirchner, J. W., Feng, Z. & Neal, C. (2000) Fractal stream chemistry and its implications for
473 contaminant transport in catchments. *Nature* **403**, 524-527.

474 Kirchner, J. W. (2003) A double paradox in catchment hydrology and geochemistry. *Hydrol.*
475 *Processes* **17**, 871-874.

476 Kirkby, M. J. (1978) *Hillslope Hydrology*. Wiley, Chichester, Great Britain.

477 Weiler, M. & McDonnell, J. J. (2007) Conceptualizing lateral preferential flow and flow
478 networks and simulating the effects on gauged and ungauged hillslopes. *Wat. Resour. Res.*
479 **43**(3), W03403, doi:10.1029/2006WR004867.

480 Loke, M. H. (2003) *Tutorial: 2-D and 3-D electrical imaging surveys*. 134 pages, URL:
481 www.geoelectrical.com.

482 McDonnell, J. J. (2003) Where does the water go when it rains? Moving beyond the variable
483 source area concept of rainfall runoff response. *Hydrol. Processes* **17**, 15, 2053-2055.

484 McDonnell, J. J. & Tanaka, T. (Eds.) (2001) *Hydrology and Biogeochemistry of Forsted*
485 *Catchments*. Special Issue of Hydrological Processes, **15**(10).

486 McDonnell, J.J. (1990) A Rationale for old water discharge through macropores in a steep, humid
487 catchment. *Wat. Resour. Res.* 26, 2821 – 2332.

488 McGuire, K. J. & McDonnell J. J. (2006) A review and evaluation of catchment transit time
489 modeling. *J. Hydrol.* **330**, 543– 563.

490 Montgomery, D. R., Dietrich, W. E., Torres, R., Anderson, S. P., Heffner, J. T. & Loague, K.
491 (1997) Hydrologic response of a steep, unchanneled valley to natural and applied rainfall.
492 *Wat. Resour. Res.*, **33**, 91-109.

493 Rubin, Y. & Hubbard S. S. (Eds.) (2005) *Hydrogeophysics*. Water Science and Technology
494 Library, vol. 50, Springer, 523 p.

495 Scherrer, S., Naef, F., Fach, A. O. & Cordery, I. (2007) Formation of runoff at the hillslope scale
496 during intense precipitation. *Hydrol. and Earth Sys. Sci.* **11**(2), 907-922.

497 Tromp-van Meerveld, H. J. & McDonnell, J. J. (2006) Threshold relations in subsurface storm
498 flow: 2. The fill and spill hypothesis. *Wat. Resour. Res.* 42, W02411,
499 doi:10.1029/2004WR003800.

500 Uhlenbrook, S., Frey M., Leibundgut, Ch. & Maloszewski, P. (2002) Residence time based

501 hydrograph separations in a meso-scale mountainous basin at event and seasonal time scales.

502 *Wat. Resour. Res.* **38**, 1-14.

503 Uhlenbrook, S. (2006) Catchment hydrology – A science in which all processes are preferential.

504 *Hydrol. Processes*, HPToday, 20, 3581-3580, DOI: 10.1002/hyp.6564.

505

506

507 **Table 1** Precipitation and discharge volumes for the investigated storm events in fall

508 1999 at both springs; uncertain values are given in brackets (see text for further details)

509

	Event 1	Event 2	Event 2a	Event 3
<i>Spring A</i>				
Precipitation (mm)	63.3	45.8	20.0	24.4
Runoff volume (m ³)	114.4	87.3	-	(0.7)
Runoff volume/precipitation (m ³ /mm)	1.81	1.91	-	(0.03)
<i>Spring B</i>				
Precipitation (mm)	62.3	49.6	12.8	49.4
Runoff volume (m ³)	111.0	85.4	7.6	61.1
Runoff volume/precipitation (m ³ /mm)	1.78	1.72	0.59	1.24

510

511

512 **Figure captions**

513 Fig. 1 Map of the test sites of hillslope A and B. The black lines show the locations of

514 the transects that were investigated using ERT (A1-A5 and B1-B4).

515 Fig. 2 Precipitation and discharge at both springs during the investigation period in fall

516 1999. Dotted lines represent interpolations of inconsistent data (due to technical

517 problems).

518 Fig. 3 Observed dissolved silica concentrations during event 1 at spring A and B;

519 concentrations were set to 100 % at the beginning of the event (equals 6.1 mg l⁻¹,

520 4.6 mg l⁻¹) to make the temporal evolution of the concentrations better

521 comparable.

522 Fig. 4 Observed concentrations of the ions sodium, chloride, potassium and sulphate

523 during event 1 at spring A and B.

524 Fig. 5 Observed deuterium signatures of spring water at spring A, B and precipitation

525 during event 1.

526 Fig. 6 Hydrograph separations using dissolved silica (spring A), and dissolved silica and

527 deuterium (spring B).

528 Fig. 7 Mixing diagram for the tracers dissolved silica and deuterium for event 1 at spring

529 B.

530 Fig. 8 Results of the 2-D electrical resistivity tomography surveys at hillslope A using

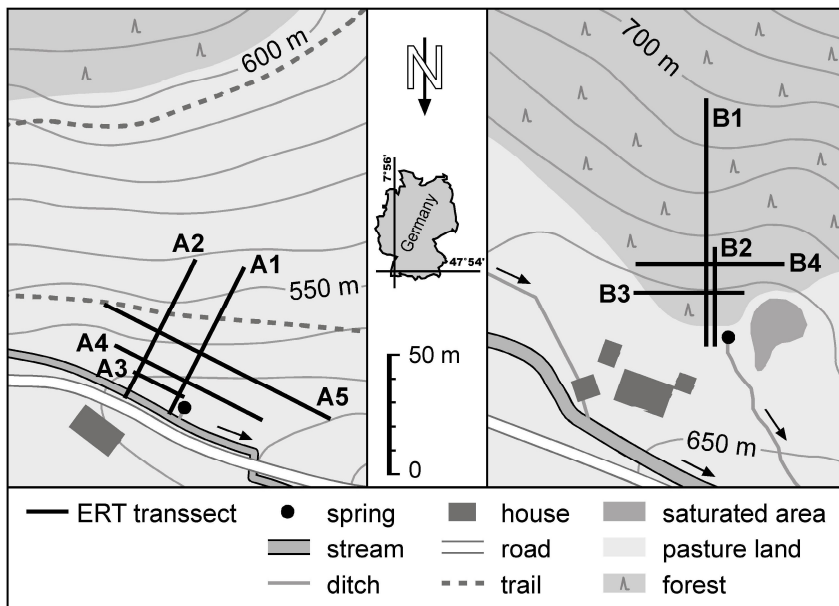
531 Wenner 2-D configurations; see Fig. 1 for the location of the transects.

532 Fig. 9 Results of the 2-D electrical resistivity tomography surveys at hillslope B using

533 Wenner 2-D configurations; see Fig. 1 for the location of the transects.

534

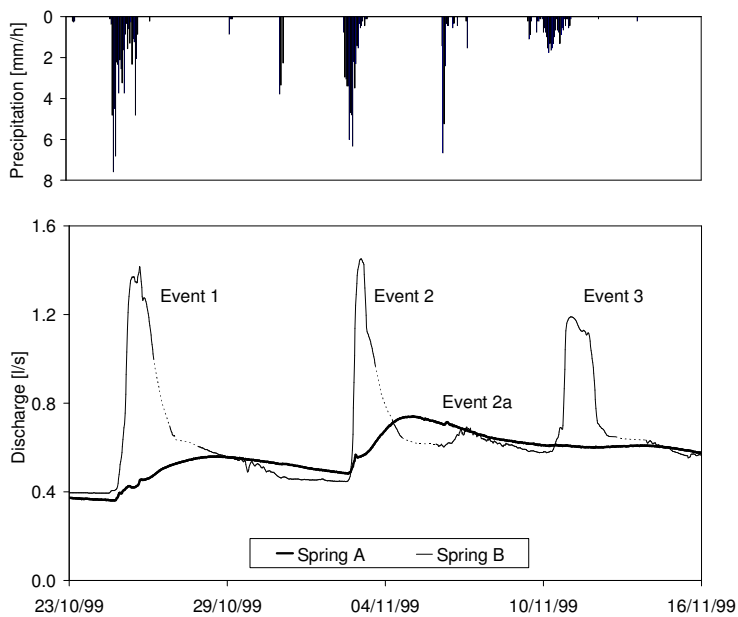
535 **Figure 1**



536

537

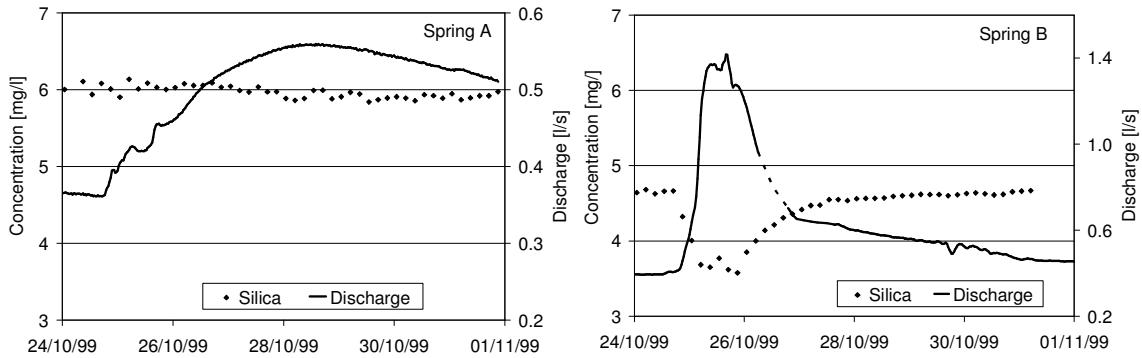
538 **Figure 2**



539

540

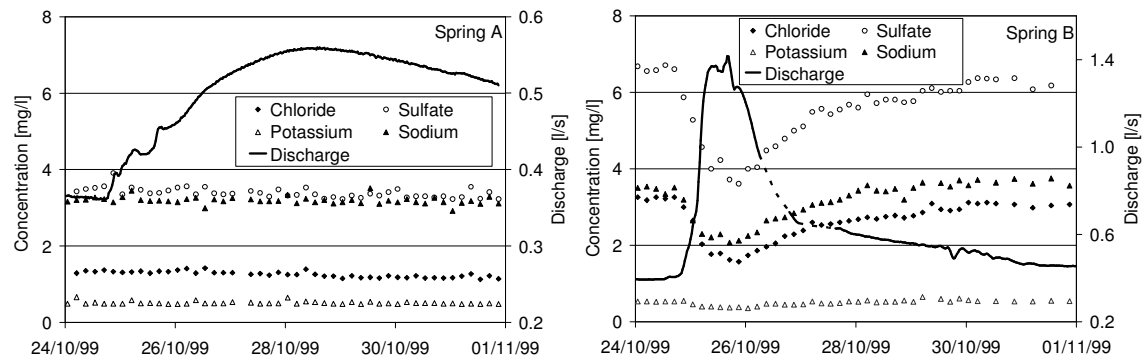
541 **Figure 3**



542

543

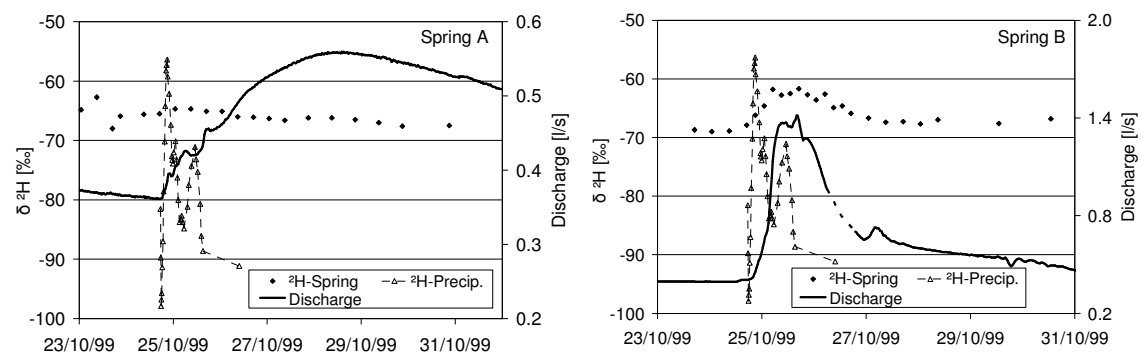
544 **Figure 4**



545

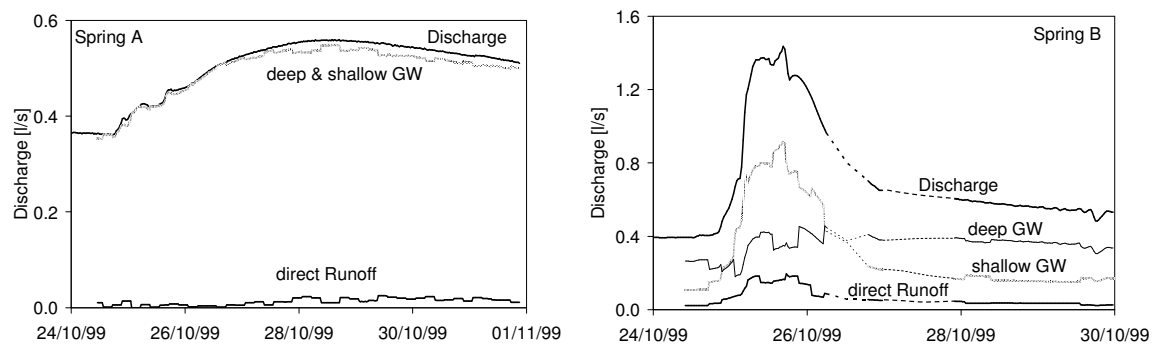
546

547 **Figure 5**



548

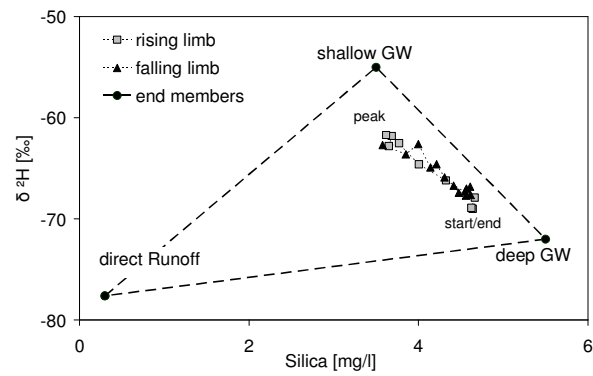
549 **Figure 6**



550

551

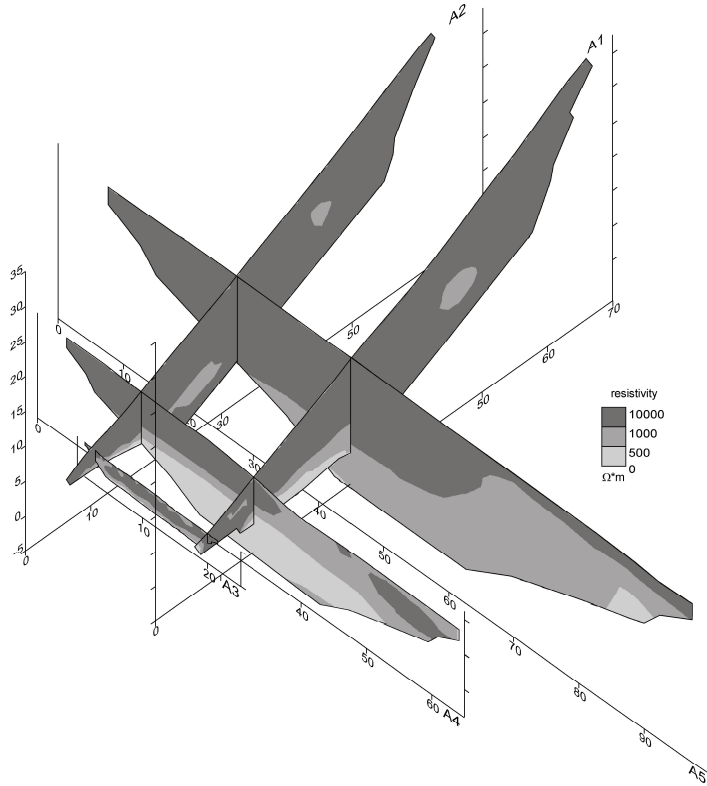
552 **Figure 7**



553

554

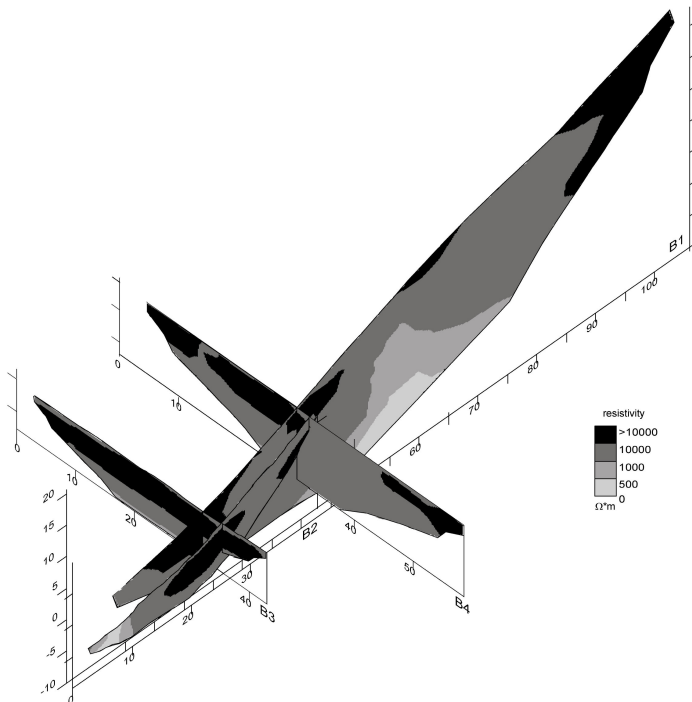
555 **Figure 8**



556

557

558 **Figure 9**



559